Journal of Alloys and Compounds, 189 (1992) 151–155
JALCOM 348

Corrosion resistance in oxygen of electrolytic nickel and cobalt phosphorus coatings

B. Gillot and K. El Amri
Laboratoire de Recherches sur la Réactivité des Solides URA 23, Faculté des Sciences Mirande, BP 138, F-21004 Dijon Cédex (France)

P. Pouderoux, J. P. Bonino and A. Rousset
Laboratoire de Chimie des Matériaux Inorganiques URA 1311, Université Paul Sabatier, 118 Route de Narbonne, F-31062 Toulouse Cédex (France)

(Received April 17, 1992)

Abstract

Corrosion of Ni–P and Co–P alloys in oxygen was investigated in the temperature range 350–800 °C on as-electrodeposited films and after annealing treatments. For as-electrodeposited films, both alloys oxidize by diffusion and the scales consist of an inner region rich in phosphorus and an outer region of oxides (NiO or Co_3O_4). Good corrosion resistance achieved after extended heating above 600 °C in vacuum, very well marked for Ni–P alloys, is explained in terms of crystallization and grain coarsening. This indicates that at these high annealing temperatures the crystals of phosphides formed a continuous layer with embedded nickel crystals rendering the alloy extremely resistant to oxygen penetration.

1. Introduction

Extensive studies have been made on the Ni–P alloys recently, particularly on the amorphous phases, because of their good corrosion resistance in environments containing a high concentration of Cl^-, NO_3^-, SO_4^- or SO_3^{2-} ions [1–5]. Coatings are amorphous when the phosphorus content exceeds 15 at.% [6–9]. Crystallization of the amorphous alloys leads to various metastable phases which are subsequently decomposed to Ni_3P and f.c.c. nickel crystals at a temperature above 650 °C. The crystallized layers are observed to yield the best corrosion resistance [3]. However, as requirements and environments change, processes which control the improved corrosion resistance must be defined for specific applications. For example, Moore and Salvati [10] have shown from microhardness tests that heat treatment at 350 °C for 1 h in air modifies the corrosion resistance of electroless nickel coatings. Moreover, with respect to the existence of nickel and Ni_3P after a prior heat treatment in vacuum below 600 °C, Lin and Lai [2] have shown that a subsequent heat treatment at temperatures above 600 °C causes grain growth and also diminishes defects. This behaviour explains the occurrence of the hardness variation in electroless Ni–P with temperature. For example, grain sizes of nickel and Ni_3P, which are smaller than 0.1 μm at 400 °C, become as large as about 3.5 μm at 800 °C.

This paper reports the results of a detailed study of corrosion resistance in oxygen of nickel– and cobalt–phosphorus alloys in the form of as-plated coatings and coatings heated in vacuum above 600 °C.

2. Experimental procedure

The Ni–P and Co–P electrodeposited coatings about 40 μm in thickness were prepared from a phosphorous acid bath [11] and nickel or cobalt sulphate and chloride. The phosphorus content was fixed by the phosphorous acid concentration in the electrolyte at a constant current density of 10 A dm^{-2}. A platinum sheet (10 cm^2) served as anode. Electrodeposition was done on copper substrates (10 cm^2) after etching in nitric acid solution. The copper base was selectively dissolved in a trichloroacetic acid and ammoniacal solution to produce a stripped coating. Then films were cut in the form of rectangular specimens measuring approximately 4×7 mm^2. The corrosion behaviour was investigated on as-deposited films and after heat treatment of the deposits under vacuum (10^{-4} Pa) in a tube furnace at temperatures ranging from 500 to 800 °C for 5 h.

Mass changes during oxidation were measured using a Setaram MTB 10-8 microbalance with a sensitivity of 10^{-3} mg. About 6 mg of rectangular specimen was placed on the balance arm, the reactor chamber was evacuated to a vacuum better than 10^{-4} Pa and the oxygen was introduced at room temperature in the case of a linear heating rate or when the proper reaction temperature was established in the case of isothermal oxidation.

Corrosion layers were analysed by means of X-ray diffraction, scanning electron microscopy, electron microprobe analysis and X-ray photoelectron spectroscopy (XPS). X-ray diffraction patterns were obtained from the face of annealed or oxidized specimens using an 'INEL' CPS-120 linear counter (curved position sensitive) with a copper or cobalt target. The morphological and energy-dispersive X-ray analyses were carried out with scale sections after mounting in a synthetic resin. X-ray photoelectron spectroscopy results were obtained using a Riber AES–ESCA–ELS MAG2 spectrometer equipped with an Al anode, which was operated at 13 kV and 20 mA current emission ($h\nu = 1486.6$ eV). Binding energies were determined using the C 1s peak at 284.6 eV.

3. Results and discussion

3.1. Non-isothermal and isothermal oxidation

The mass gain–phosphorus content curves $\Delta m/S = f(\text{at.\%P})$ (where S represents the surface area) observed during the oxidation of Ni–P and Co–P alloys at various temperatures for as-deposited films are shown in Figs. 1 and 2 respectively. These curves are obtained from the $\Delta m/S = f(T)$ curves during continuous heating at a constant rate of 2 °C min^{-1}. In both cases the reaction starts at about 350 °C and presents two distinct zones, particularly marked at higher oxidation temperatures. The first zone of low phosphorus content corresponds approximately to alloys having phosphorus-supersatured solid solutions of crystalline nickel or cobalt whose grain size decreases with increasing phosphorus concentration [12]. We can imagine that in this region below the eutectic composition the reactivity depends strongly on the crystallite size of the metal and that the increase in mass gain can be attributed to the precipitation of fine nickel or cobalt particles as a major constituent in the as-deposited state when the phosphorus content increases.

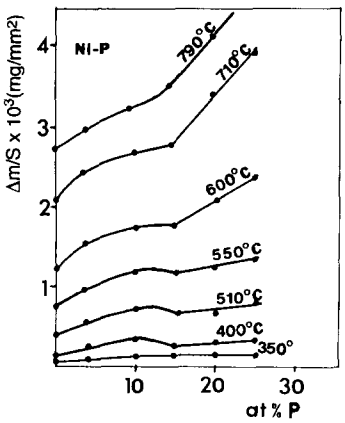

Fig. 1. Mass gain *vs.* at.% P at various temperatures for as-deposited Ni–P alloys.

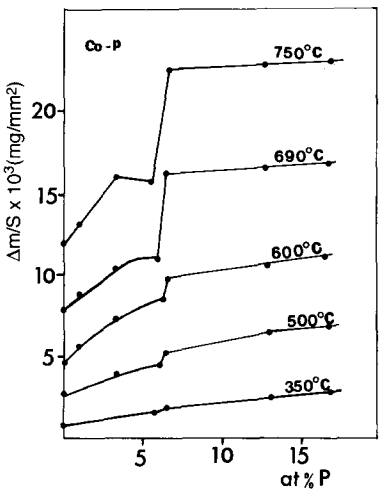

Fig. 2. Mass gain *vs.* at.% P at various temperatures for as-deposited Co–P alloys.

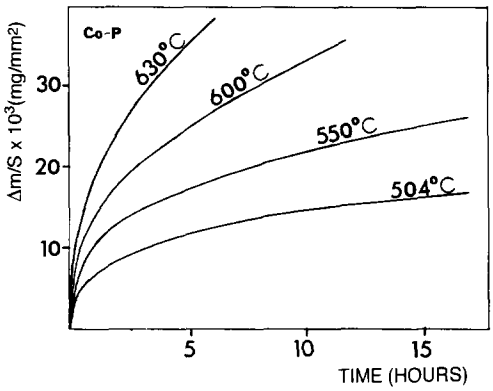

Fig. 3. Mass gain *vs.* time for as-deposited Co–P alloys with 12.4 at.% P.

The second zone forms differently with the metal matrix. For Ni–P deposits containing high phosphorus contents (greater than 15 at.%P) the mass gain increases linearly with phosphorus content, whereas for Co–P deposits (greater than 6.2 at.% P) the mass gain increases more slowly. We can imagine that in this region, heating in oxygen at a linear rate of 2 °C min^{-1} without isothermal annealing at elevated temperature causes a different behaviour in the crystallization process.

The mass gain–time curves $\Delta m/S = f(t)$ are shown in Figs. 3 and 4 for various temperatures. The protective

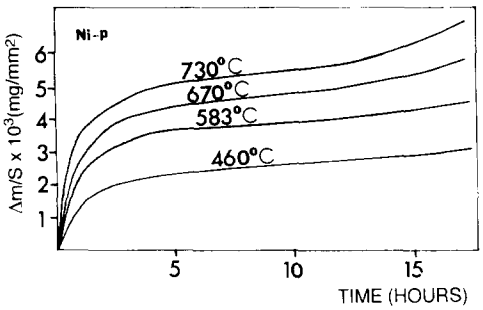

Fig. 4. Mass gain *vs.* time for as-deposited Ni–P alloys with 22 at.% P.

TABLE 1. Activation energies for Co–P and Ni–P alloys

Co–P		Ni–P	
P (at.%)	E (kJ mol^{-1})	P (at.%)	E (kJ mol^{-1})
0	96	0	177
1	104	10	154
6.5	167	15	192
12.4	146	25	200

nature of the reaction is evident. It was found to follow a parabolic law at all temperatures and phosphorus contents for Co–P deposits as indicated by the linearity of mass gain squared per unit area *vs.* exposure time. In the case of Ni–P deposits we observe the presence of two parabolic stages for each curve, the first being faster. For long reaction times (greater than 10 h) and owing to the form of the kinetic curves we have to state that the scales were detached from the substrate, occurring again on an increase in the reaction rate. The temperature-dependent parabolic rate signifies that a diffusion-controlled process is rate determining. Such a process may include diffusion of the reactants through the growing impact scale (Wagner mechanism) or diffusion of the oxidant to the metal–scale interface. We can imagine, depending on experimental conditions, that when the MO–O_2 equilibrium is established the M oxide forms at the outer-scale surface with nickel or cobalt diffusion through the oxide scale. Activation energies (E) calculated from the slopes of straight lines $(\Delta m/S)^2 = f(t)$ are given in Table 1. These activation energies for as-deposited films without phosphorus are in good agreement with those reported previously for pure metals [13].

We have plotted in Figs. 5 and 6 the mass gain $\Delta m/S$ *vs.* T at different annealing temperatures (T_a). Results clearly show that for Ni–P and Co–P deposits with a high phosphorus content the mass gain strongly decreases between 500 and 750 °C, which implies good corrosion resistance and probably indicates a sequence of microstructure changes. This behaviour contrasts with that of deposits with a low phosphorus content,

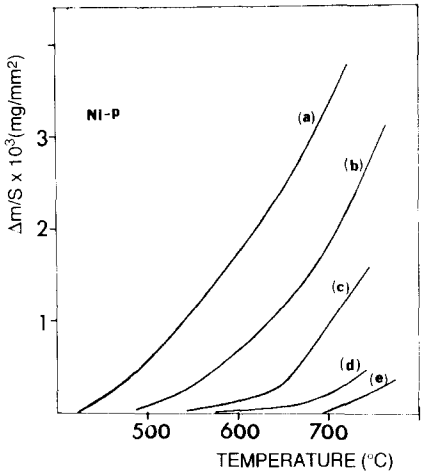

Fig. 5. Temperature dependence of mass gain in Ni–P alloy with 25 at.% P for several annealing temperatures T_a: (a) as deposited, (b) 650 °C, (c) 700 °C, (d) 750 °C, (e) 800 °C.

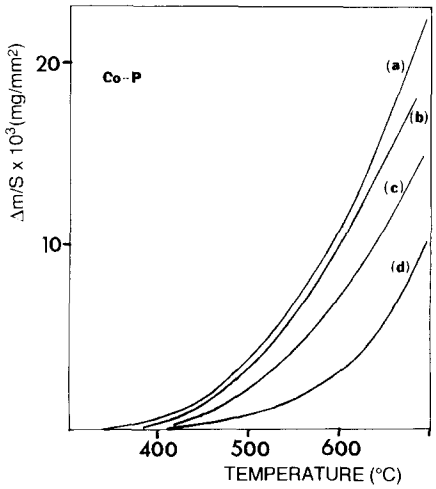

Fig. 6. Temperature dependence of mass gain in Co–P alloy with 12.4 at.% P for several annealing temperatures T_a: (a) as deposited, (b) 500 °C, (c) 650 °C, (d) 750 °C.

where the effect of the annealing temperature on the mass gain was only slight and afforded little protection against oxidation.

3.2. *Phase identification*

The X-ray patterns for phases present after annealing treatment under vacuum and for oxidation reaction products are obtained directly on the scales. The as-deposited coating with high phosphorus content (Figs. 7 and 8, curves (a)) has a diffraction pattern consisting of one large broad peak which is characteristic of an amorphous material. When the sample was annealed at 700 °C, a large number of reflection peaks emerged (Figs. 7 and 8, curves (b)), indicating the presence of phases very well crystallized. These were indexed as Ni_3P and nickel crystalline phases for Ni–P alloys and cobalt phosphide (Co_2P and CoP) and cobalt crystalline

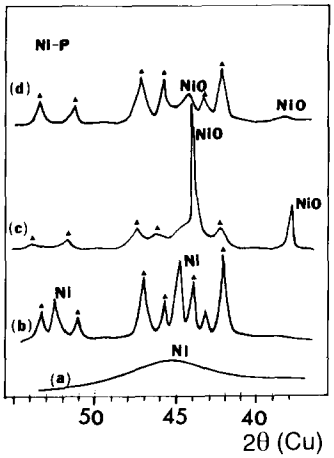

Fig. 7. X-ray diffraction patterns of Ni–P alloys (22 at.% P) heated under various content (▲, Ni_3P): (a) as deposited, (b) annealed at 700 °C for 5 h, (c) oxidized at 700 °C without annealing, (d) annealed and oxidized at 700 °C.

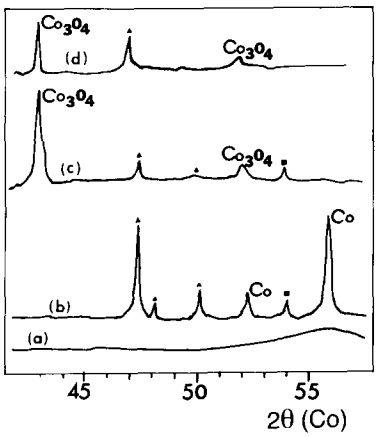

Fig. 8. X-ray diffraction patterns of Co–P alloys (12.4 at.% P) heated under various conditions (▲, Co_2P; ■, CoP): (a) as deposited, (b) annealed at 700 °C for 5 h, (c) oxidized at 700 °C without annealing, (d) annealed and oxidized at 700 °C.

phases for Co–P alloys, although in general rather poor X-ray patterns were obtained for cobalt phosphides. For the cobalt-based alloy it has been shown that phosphorus is segregated to the grain boundaries [14]. It has also been postulated that for these high annealing temperatures, Ni_3P and cobalt phosphides are the matrix phases after heating at 700 °C [2, 3], whereas the matrix for the low phosphorus alloys is the metal phase. Moreover, the appearance of more than two transformation peaks in differential scanning calorimetry [8] for Ni–P alloys may be considered to be a phenomenon caused by a large difference in phosphorus concentration across the layer thickness. When the as-deposited alloys were heated, without prior annealing, in oxygen at 700 °C (Figs. 7 and 8, curves (c)), the nickel and cobalt phases disappeared and NiO and Co_3O_4 oxides were observed, with little of phosphide phase detected for the Ni–P alloy. After annealing and oxidation at the same temperature (Figs. 7 and 8, curves (d)), crystallized Ni_3P and Co_2P phases still persisted in the scale but the intensity of the peaks corresponding to oxides diminished strongly, indicating that only minor amounts of NiO and Co_3O_4 were formed.

3.3. Analysis of corrosion layers

At temperatures ranging from 600 to 800 °C and after oxidation without annealing, the cross-section of the scale revealed that for Ni–P alloys the scale consisted of two layers: an inner layer enriched in phosphorus and an outer layer of NiO with no appreciable phosphorus at the solid–gas interface. For Co–P alloys morphological observations showed that the scale that formed probably consisted of two oxide layers with CoO inside, containing a uniform distribution of phosphorus or phosphides of cobalt and Co_3O_4 outside. Indeed, electron microprobe analysis (Fig. 9) revealed that in both cases the phosphorus was concentrated next to the substrate whereas the compact oxide was completely free from phosphorus. After annealing and oxidation at 700 °C, the scales formed on the alloys were complex and modified with oxidation temperature. They generally consisted of duplex layers which contained mainly metal oxides with an appreciable amount of phosphide phases. An X-ray spectrum of the scale shows primarily nickel or cobalt and phosphide in the outer layer with an enrichment of phosphorus at the metal–alloy interface.

This is confirmed by XPS analyses. XPS of as-deposited films for the Ni 2p and P 2p lines (Fig. 10, curve (a)) exhibits peaks due to Ni^0 (851.8 eV), $Ni(OH)_2$ (856.7 eV), P^0 (129.2 eV) and PO_4^{3-} (129.7 eV). It is significant that no oxides were detected on the surface and that in the phosphorus-rich region free phosphorus and phosphides are difficult to distinguish, probably because the shift in the binding energy is quite small [15]. Spectra after heat treatment in oxygen at 700 °C (Fig. 10, curve (b)) show the presence of only NiO (855.6 eV), with the surface free of any phosphorus

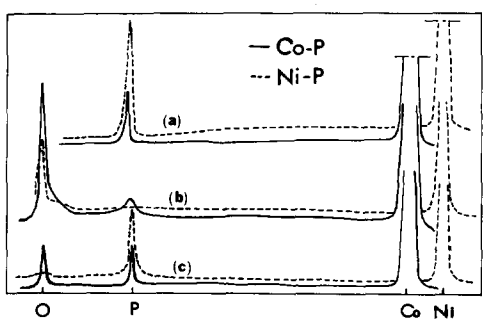

Fig. 9. Energy-dispersive X-ray spectrum of Ni–P (25 at.% P) and Co–P (12.4 at.% P) alloys: (a) at the outer surface for as-deposited alloy, (b) after oxidation at 700 °C at the gas–oxide interface, (c) after oxidation at 700 °C at the metal–oxide interface.

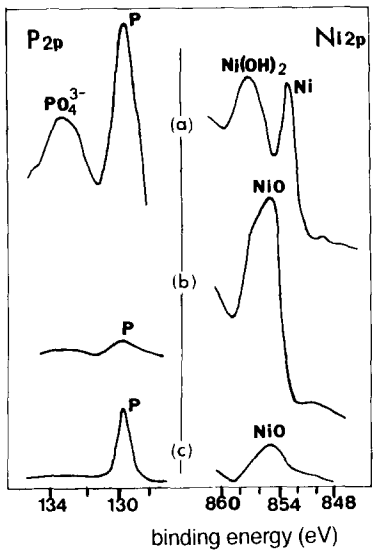

Fig. 10. Characteristic Ni 2p and P 2p spectra for alloy with 25 at.% P: (a) as deposited, (b) after oxidation at 700 °C, (c) after annealing and oxidation at 700 °C.

compound. After annealing and oxidation at the same temperature, NiO and phosphorus were present at the alloy surface as confirmed from morphological observations. The Co 2p and P 2p spectra of the Co–P alloy show a similar behaviour for as-deposited and oxidized films with or without annealing.

4. Summary and conclusions

The oxidation resistance of Ni–P and Co–P alloys heated at higher temperatures under non-isothermal conditions is little affected by their phosphorus content. In the presence of oxygen it appears that the amount of precipitates formed from amorphous phases depends more strongly on the annealing time imposed at every moment to the sample. It is however limited by the heating rate of 2 °C min^{-1} used.

Oxide growth under isothermal conditions on as-deposited Ni–P and Co–P alloys with various percentage of phosphorus was parabolic, indicating oxidation protection behaviour. Diffusion through the oxide scale after a short period becomes the reaction's rate-determining step. Thus the mechanism for the growth of the oxide outer layer involves metal diffusion outwards from MO/M–P to the O_2–MO interface. This explains the metal depletion which subsequently leads to the formation of an inner region enriched in phosphorus.

However, the most significant feature of this work is to clarify the way in which annealing in vacuum in the range 600–800 °C is found to improve the corrosion resistance to oxygen of Ni–P and Co–P alloys with high phosphorus content. We suggest that prior heating in vacuum at high temperatures for a long period (5 h) produces a continuous layer of phosphides with embedded metal crystals which permits the protection of alloys against high temperature corrosion.

References

1 Q. X. Mai, R. D. Daniels and H. P. Harpalani, *Thin Solid Films, 166* (1988) 235.
2 K. L. Lin and P. J. Lai, *J. Electrochem. Soc., 136* (1989) 3803.
3 G. H. Schenzel and H. Kreye, *Plat. Surf. Finish., 77* (1990) 50.
4 K. S. Rajam, I. Rasągopal and S. R. Rajagopalan, *Met. Finish., 27* (1990) 77.
5 M. L. Sui, S. Patu and Y. Z. He, *Scr. Metall., 23* (1991) 1537.
6 E. M. Ma, S. E. Luo and P. X. Li, *Thin Solid Films, 166* (1988) 273.
7 R. C. Agarwala and S. Ray, *Z. Metallk., 80* (1989) 556.
8 K. H. Hur, J. E. H. Jeong and D. N. Lee, *J. Mater. Sci., 25* (1990) 2573.
9 A. H. Graham, R. W. Lindsay and H. J. Read, *J. Electrochem. Soc., 112* (1965) 401.
10 R. L. Moore and L. Salvati Jr., *Thin Solid Films, 193–194* (1990) 270.
11 P. Pouderoux, I. Chassaing, J. P. Bonino and A. Rousset, *Surf. Coat. Technol., 45* (1991) 161.
12 E. Vafaei-Makhsoos, E. L. Thomas and L. E. Toth, *Metall. Trans. A, 9* (1978) 1449.
13 J. Benard, *L'Oxydation des Métaux*, Gauthier-Villard, Paris, 1982.
14 K. Hono and D. E. Laughlin, *J. Magn. Magn. Mater., 80* (1989) L137.
15 C. D. Wagner, W. M. Riggs, L. E. Davis, J. F. Moulder and G. E. Muilenberg (eds.), *Handbook of X-ray Photoelectron Spectroscopy*, Perkin-Elmer, Palo Alto, CA, 1978.